Saudi Pharmaceutical Journal 30 (2022) 946–953

Contents lists available at ScienceDirect

Saudi Pharmaceutical Journal

journal homepage: www.sciencedirect.com

Original article

Preparation and characterization of Meta-bromo-thiolactone calcium alginate nanoparticles

Esra Kamal Eltayb [a], Fadilah Sfouq Aleanizy [a,*], Fulwah Y. Alqahtani [a], Hamad M. Alkahtani [b], Siddique Akber Ansari [b], Ibrahim Alsarra [a]

[a] Department of Pharmaceutics, College of Pharmacy, King Saud University, P.O. Box 22452, Riyadh 11495, Saudi Arabia
[b] Department of Pharmaceutical Chemistry, College of Pharmacy, King Saud University, P.O. Box 2457, Riyadh 11451, Saudi Arabia

ARTICLE INFO

Article history:
Received 13 April 2022
Accepted 20 May 2022
Available online 23 May 2022

Keywords:
Calcium alginate
Meta-bromo-thiolactone (mBTL)
Pseudomonas aeruginosa
Alginate nanoparticles

ABSTRACT

Recently, the focus has been shifting toward Quorum sensing inhibitors which reduce Pseudomonas aeruginosa virulence factors, alleviating infections. In this work, me-ta-bromo-thiolactone (mBTL), a potent quorum and virulence inhibitor for the *Pseudomonas aeruginosa* strains, were formulated in calcium alginate nanoparticles (CANPs). Alginate is used as nutrients and as backbone virulence aspect for Pseudomonas and therefore was chosen. mBTL-loaded-CANPs were characterized for particle size, polydispersity index, zeta potential, morphology visualized by Transmission Electron Microscopy (TEM) and drug release profile. Chemical and physical analysis of formulated mBTL-loaded-CANPs were evaluated using Fourier transform infrared Spectroscopy (FTIR) and differential scanning calorimetry (DSC) and Physical stability of mBTL-loaded-CANPs assessed at various temperature 25 ± 1 °C, 4 ± 0.5 °C and −30° ± 1 °C over a period of 4 and 9 months. Synthesized CANPs showed nano-size particles ranging from 140 to 200 nm with spherical particles for plain CANPS and irregular shape for mBTL-loaded-CANPs with a sustainable release profile over 48hrs. FTIR showed stable structure of loaded-mBTL and DSC displayed no interaction between mBTL and polymer. State of released mBTL from CANPs kept at 25 °C, 4 °C and −30 °C over 4 and 9 months showed stable formula at room temperature which kept as a goal of nanoparticles storage. The findings of this study revealed successful preparation of mBTL-loaded-CANPs.

1. Introduction

Pseudomonas aeruginosa is a widespread opportunistic pathogen that is predominant in soil and water and can infect patients with preexisting conditions, as immunosuppression, wounds, burns, or indwelling medical devices. *P. aeruginosa* was found to be a major lung infectious pathogen in cystic fibrosis (CF) patients (Gellatly and Hancock, 2013). *P. aeruginosa* possesses a large number of genes that are involved in regulation, and controlling their virulence which can be attributed to the remarkable ability of this bacterium to adapt a wide range of environmental niches (Lee et al., 2006). *P. aeruginosa* not only secrete alginate as a major virulence factor but also alginate can be utilize as nutritional material (Monday and Schiller, 1996). There are several advantages that alginate confers on *P. aeruginosa* as facilitating cells attachments and colonization and protects *P. aeruginosa* from phagocytic clearance and shields them by scavenging the free radicals released by the activated macrophages (Govan and Deretic, 1996). In addition, alginate enhances fighting to antimicrobial agents by deterring the passage of these compounds to the bacteria, by binding the compounds and/or by deactivating them (Bayer et al., 1991, Bayer et al., 1992). There are a number of studies indicating that the biofilm formation and structure in different *P. aeruginosa* species affected by alginate overproduction (Baselga et al., 1993, Yildiz and Schoolnik, 1999, Danese et al., 2000).

The emergence of antibiotic-resistant strains of *P. aeruginosa* is a major concern in public health and is associated with high mortality rate (Gellatly and Hancock, 2013). Virulence and colonization as well as multidrug-resistant behavior in *P. aeruginosa* controlled by quorum sensing (QS) which is the cell-to-cell communication

* Corresponding author.
E-mail address: faleanizy@ksu.edu.sa (F.S. Aleanizy).
Peer review under responsibility of King Saud University.

Production and hosting by Elsevier

https://doi.org/10.1016/j.jsps.2022.05.008
1319-0164/

that can be regulated by using small molecules known as quorum sensors inhibitors (Hentzer et al., 2003, Amara et al., 2009, O'Loughlin et al., 2013). Previous study has reported that synthetic molecules *meta*-bromo-thiolactone (mBTL) have inhibited *P. aeruginosa* QS receptors LasR and RhlR (O'Loughlin et al., 2013) and provide the uppermost activity of inhibition of QS system. The mBTL is the most potent compound against *P. aeruginosa* bacteria (Smith and Iglewski, 2003, O'Loughlin et al., 2013), not only prevents virulence factor expression and biofilm production but also protects *Caenorhabditis elegans* and human A549 lung epithelial cells from QS–mediated killing *by Pseudomonas strain* (O'Loughlin et al., 2013). Their findings demonstrated the potential therapeutic utilization of mBTL as a modulator of quorum sensing. Taking into considerations that mBTL is a very potent QS inhibitor, and more importantly the ability of this bacterium to secrete and use alginate; it was proposed that a successful generation of calcium alginate loaded mBTL nanoparticles would facilitate the mBTL uptake by the *P. aeruginosa*.

2. Materials and methods

2.1. Chemicals

Compound 4-(3-bromophenoxy)-*N*-(2-oxotetrahydrothiophen-3-yl)butanamide (mBTL) (Fig. 1) was synthesised according to the procedure described previously (O'Loughlin et al., 2013).

2.2. Preparation of calcium alginate nanoparticles (CANPs) and loading CANPs with mBTL

The CANPs prepared in this study were synthesized using emulsification method (Christiani et al., 2016). Sodium alginate solution of concentration 2% w/v was prepared by dissolving sodium alginate in deionized water. Sodium alginate solution was homogenized using a mechanical stirrer at 1300 rpm for 30 min, then Tween 20 and canola oil were added to produce the desired emulsion. Calcium chloride at a concentration of 2% w/v was added dropwise to the emulsion at a flow rate of 0.01 ml/s to produce the desired calcium alginate nanoparticles. The emulsification system was left at 1 h for Ca^{2+} crosslinking at water/oil interface. The pellet of CANPs were collected by high centrifugation using minicentrifuge (Fisher 05–090-100,UK) at 14000 rpm for 30 min at 4 °C. The nonformula was re-suspended in acetone (1:0.5) followed by centrifugation at 14000 rpm for 15 min at 4 °C to remove residual canola oil and tween 20 also, for cleaning, precipitation and dehydration to form white pellet CANPs (Christiani et al., 2016). For loading mBTL, it was added at 0.4% w/v into aqueous sodium alginate and was emulsified after tween 20 and canola oil were added and followed for preparation of drug loaded CANPs.

2.3. Measurement of Nanoparticle size and Zeta potential (ζ potential)

The average particle size (PS), surface charge existent on CANPs, and polydispersity (PDI) index were determined (in triplicate) using a zetasizer, (Nano ZS90 Malvern Instruments Ltd, UK) at 25 °C at a 90°scattering angle, and was analyzed by 'DTS nano' software (Liu et al., 2018).

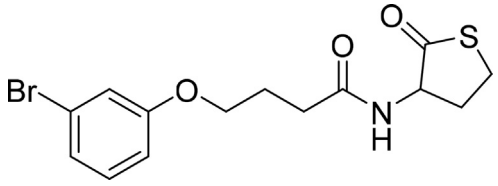

Fig. 1. Chemical structure of 4-(3-bromophenoxy)-*N*-(2-oxotetrahydrothiophen-3-yl)butanamide (mBTL).

2.4. Transmission electron Microscopy (TEM)

Morphology of CANPs was visualized and determined of particle diameter using TEM (Li et al., 2008). A drop of CANPs formulation was placed onto grid after suitable dilution. The grid was air dried after excess formulation was removed using filter paper within 10 min, then image of vesicles was taken and analyzed via JEM-1400, JEOL (Tokyo, Japan).

2.5. Determination of mBTL-loaded CANPs encapsulation efficiency (EE %)

The encapsulation efficiency (EE%) of the mBTL-loaded CANPs formulation was determined by indirect method (Yan et al., 2020). Briefly, after preparing of fresh mBTL-loaded CANPs it was separated from aqueous medium containing free mBTL in supernatant by centrifugation at 14000 rpm for 30 min at 4 °C. After a suitable dilution with distilled water, the amount of free mBTL in supernatant was analyzed by UV–Visible/spectrophotometric at λ_{max} 280 nm (Biochrome libra S22, Thermo-Fisher Scientific, Waltham MA, USA). The encapsulation efficiency was determined as follows:

$$\text{EE}\,(\%) = \frac{\text{Total amount of mBTL} - \text{amount of the free mBTL}}{\text{Total amount of drug}} \times 100$$

2.6. In vitro release of mBTL-loaded CANPs

The in vitro drug release from CANPs formulation was carried out using dialysis technique (Thomas et al., 2019). Dialysis cellulose membrane with a molecular weight cut-off (MWCO) 14 K Dalton (Da) was soaked in phosphate buffered saline (PBS). Aliquots (1 ml) of mBTL-loaded CANPs (containing 4 mg/ml of mBTL) was placed in the membrane. Then dialysis membrane was suspended in 50 ml beaker containing 30 PBS (pH 7.4). The test was performed using shaker water bath at 100 rpm at 37 ± 0.5 °C. The samples were withdrawn at per-determined time intervals (0.5, 1,2,3,4,5,6,7,8,24, and 48 h) and replaced by PBS (pH 7.4) solution, and the mBTL content calculated.

2.7. Fourier transform infrared Spectroscopy (FTIR)

IR spectrum was performed by Perkin Elmer FTIR Spectrum BX apparatus (Perkin Elmer, USA) in Chemistry Department, College of science, King Saud University. The structural composition of prepared nanoparticles was analyzed by FTIR (Sarmento et al., 2006, Gomathi et al., 2017). The FTIR spectra of sodium alginate powder, calcium chloride powder, Pure mBTL, lyophilized plain CANPs and lyophilized mBTL-loaded CANPs were prepared by conventional potassium bromide (KBr) disc method (2 mg sample in 98 mg KBr) and examined in the transmission mode. KBr disc was prepared at pressure of 10 ton. The wavelength range for IR scan was from 4000 to 400 cm^{-1} at a resolution of 2 cm^{-2} and the different wavelengths of the spectrum was recorded and compared to literature to determine the different functional groups in samples.

2.8. Differential scanning calorimetry (DSC)

Thermal analysis of Physical mixtures of CANPs components (sodium alginate and calcium chloride), pure mBTL, plain CANPs and mBTL-loaded CANPs were recorded and performed using DSC

analysis (Perkin Elmer, USA) in the Research Center, College of Pharmacy, King Saud University, Saudi Arabia. The tested samples equivalent to 2–2.5 mg were placed and sealed in an aluminium DSC pan. Then, each sample was heated from 30 to 300 °C at a rate of 10 °C/min individually under N2 atmosphere (50 ml/min flow rate). Blank aluminium pan was used as a reference (Sarmento et al., 2006, Bhatt et al., 2020).

2.9. Stability test

Particle size, PDI and ζ *potential are* the key parameter used to evaluating the physical stability of formulated CANPs under different temperature conditions at room temperature 25 ± 1 °C, 4 ± 0.5 °C and −30° ± 1 °C. The samples were tested at predetermined time intervals,4 months and 9 months (Libo et al., 2011).

3. Results

3.1. Characterizing mBTL-loaded calcium alginate nanoparticles CANPs

The plain CANPs and mBTL-loaded CANPs were prepared via emulsification technique and were characterized with respect to PS, PDI and ζ potential. Table 1 shows homogenized NPs with PS of 141.1 ± 3.08 nm and 175.4 ± 7.25 nm with ζ potential of −21.1 mv ± 0.571 and −45.7mv ± 0.920 for plain and mBTL-loaded CANPs, respectively.

Morphology and shape of plain and mBTL-loaded CANPs were visualized using TEM. TEM revealed that the plain CANPs was spherical in shape with a size between 99 and 454 nm (Fig. 2A). On the other hand images of mBTL loaded CANPs showed spherical, geometrical and irregular particles within the size range of 154–512 nm (Fig. 2B). The enlargement of the particles attributed to encapsulating mBTL molecules.

Table 1
This is a table. Tables should be placed in the main text near to the first time they are cited.

Nanoparticle	PS diameter (nm) ± SD	PDI ± SD	Zeta potential (mv) ± SD
Plain CANPs	141.1 ± 3.08	0.34 ± 0.020	−21.1 ± 0.571
mBTL loaded CANPs	175.4 ± 7.25	0.4 ± 0.026	−45.7 ± 0.920

3.2. Determination of mBTL encapsulation efficiency (EE%)

mBTL encapsulation determination is a method to assess the ability of CANPs to mBTL encapsulation. The indirect method was used to determine the percentage encapsulation efficiency (EE%) of the mBTL in CANPs and it was validated based on calibration curve of mBTL. The percentage of fresh mBTL encapsulated inside CANPs was 93.21% ± 0.045 and measurement was achieved in triplicate.

3.3. In-vitro release of free-mBTL and mBTL-loaded CANPs

In-vitro release of free mBTL and mBTL-loaded CANPs in 30 ml PBS buffer of pH 7.4 at 37 ± 0.5 °C, over 48 h as a time function were performed using dialysis membrane. The concentration of free mBTL and mBTL-loaded CANPs were analyzed by UV–visible spectrophotometer assay to calculate of mBTL absorbance at 280 nm. The mBTL release profile through the membrane was characterized by a sustained flow pattern either free or loaded in CANPs. The percentage release of the free mBTL was 100 % ± 0.015 diffused through membrane within 7 h. While the percentage release of the mBTL from CANPs through 24 h was 80.13 ± 0.034. Then, the mBTL release was gradually increased to 95.27 ± 0.032 by diffusing through membrane within 48 h. The in vitro drug release profiles obtained for free mBTL and mBTL-loaded CANPs were shown in Fig. 3.

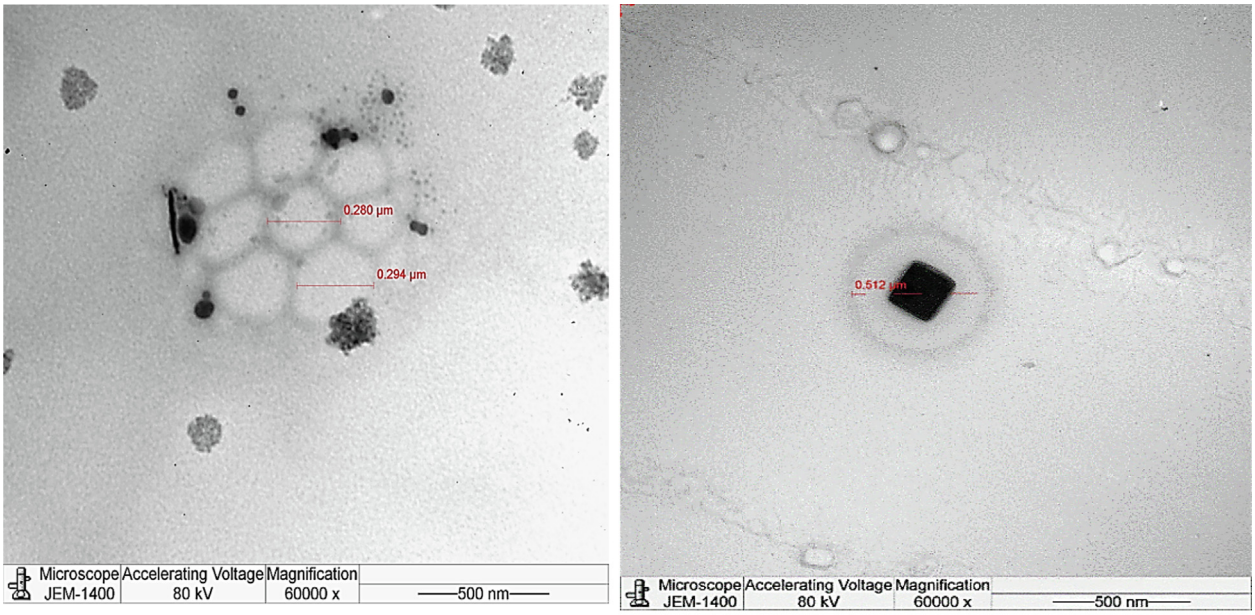

Fig. 2. Morphological study of CANPs either plain or loaded visualized using transmission electron microscope (TEM). (a) TEM image of plain CANPs; (b) TEM image of mBTL loaded CANPs.

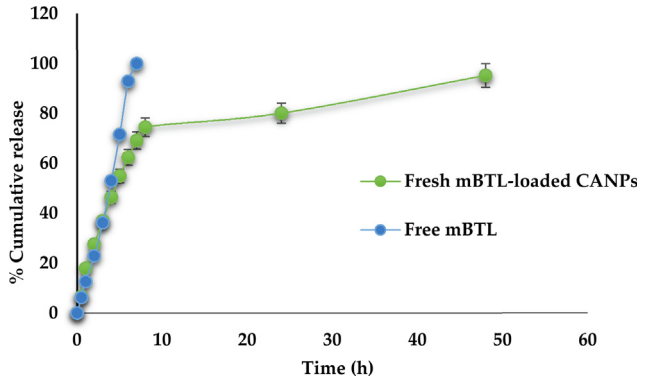

Fig. 3. The in-vitro release profile of free mBTL and fresh mBTL-loaded CANPs were evaluated in PBS buffer of pH 7.4 at 37 ± 0.5 °C. Points represent averages ± SD.

3.4. Chemical analysis of mBTL-loaded CANPs

3.4.1. Fourier transforms infrared Spectroscopy (FTIR)

FTIR spectra of sodium alginate, calcium chloride, free mBTL, plain CANPs and mBTL-loaded CANPs were shown in Fig. 4. Based on FTIR spectra findings, a minor difference was seen in the width and frequency of the peaks revealing absorption bands of hydroxyl and carbonyl functional groups. The FTIR spectra of sodium alginate showed a strong and broad peak in the 3428.06 cm^{-1} corresponding to O—H stretching vibration and —CH vibration band at 2930.77 cm^{-1} at spectrum of sodium alginate. Observed bands at 1620.03 cm^{-1} were related to the stretching vibrations of the carboxylate salt ion (COO– groups). At FRIR spectra of plain CANPs was shifted to minor lower wavelength number to 3403.98 cm^{-1} due to presence of hydroxyl group and carboxylate group of sodium alginate to the ion of calcium to form chelating structure and then decrease in hydrogen bond between hydroxyl function groups. The stretching vibrations of the carboxylate salt ion (COO— groups) in sodium alginate shifted to higher wavelength numbers because calcium ion was replaced sodium ions in the sodium alginate that lead to charge density was changed and hence, this shifting should be expected and at 1745.77 cm^{-1} corresponding to stretching ester. The FTIR spectra of free mBTL was showed peaks in the 3287.69 cm^{-1} and 3055.16 cm^{-1} corresponding to N—H and C—H aromatic stretching vibration, respectively and at 2928.59–2870.22 cm^{-1}, were attributed to stretching vibration of —CH_3 -aliphatic group. The C=O amide and C=O thiolactone stretching vibration bands at 1648.22 cm^{-1} and 1692.86 cm^{-1} were observed in spectra of mBTL. Other wavelength number in mBTL corresponding to certain function groups such as 2510.83 cm^{-1}, 1462.39 cm^{-1}, 1325.29 cm^{-1} and 1223.80 cm^{-1} were attributed to stretching vibrations of S—H thiol, C—S, C—O and C—N groups. At FTIR spectra of mBTL-loaded CANPs, the absorption region of stretching vibration of O-H bond in calcium alginate appeared broad band lead to masking wavelength number of N-H stretching vibration of mBTL. The wavelength number at 1656.66 cm^{-1} corresponding to thiolactone ring stretching vibration in mBTL and appeared in mBTL-loaded CANPs.

3.4.2. Differential scanning calorimetry (DSC)

The thermal properties of free mBTL, calcium chloride, sodium alginate, plain CANPs and the physical mixture of mBTL-loaded CANPs were determined using differential scanning calorimetry (DSC). DSC measures endothermic and exothermic transitions such as melting and crystallization as a function of temperature. It gives information about the physical state of drug in the calcium alginate nanoparticles and predicting of an interaction between the drug and polymer. In Fig. 5, which show initial two endothermic peaks at 96.27 °C, 146.82 °C of calcium chloride and one endothermic peak at 85.11 °C. The thermogram of mBTL showed a characteristic sharp exothermic single peak around 91 °C also, the endothermic peak of physical mixture appeared to be combination of calcium chloride and sodium alginate was registered at 140.47 °C. The free mBTL peak was appeared and distinguished in thermogram of mBTL-loaded CANPs and increase in melting point of free mBTL

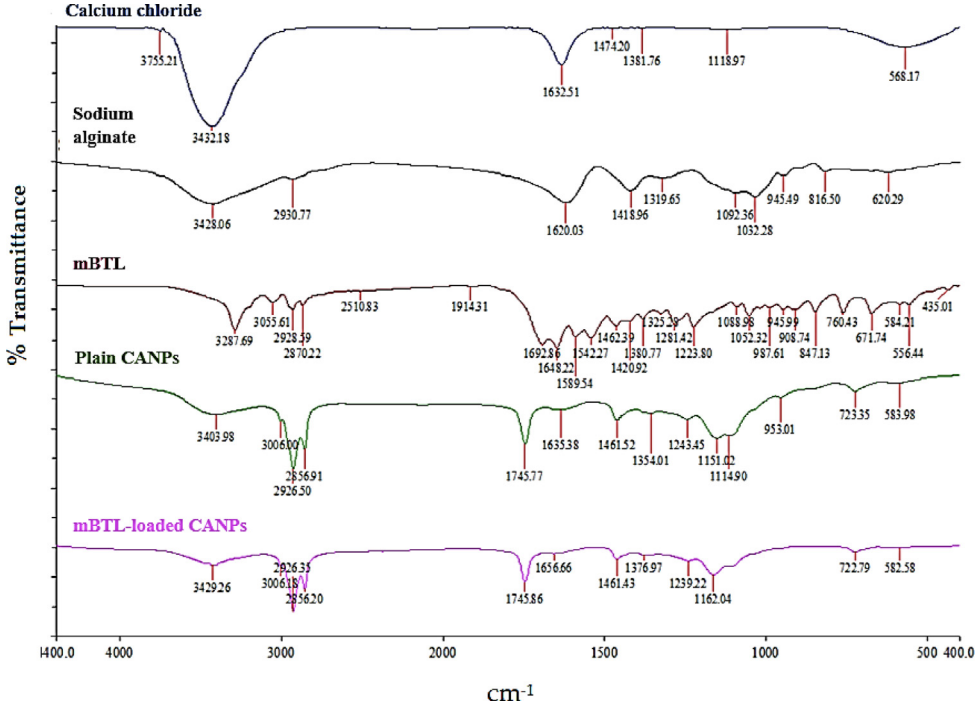

Fig. 4. The FT-IR spectra of calcium chloride, sodium alginate, free mBTL, plain CANPs and mBTL-loaded CANPs.

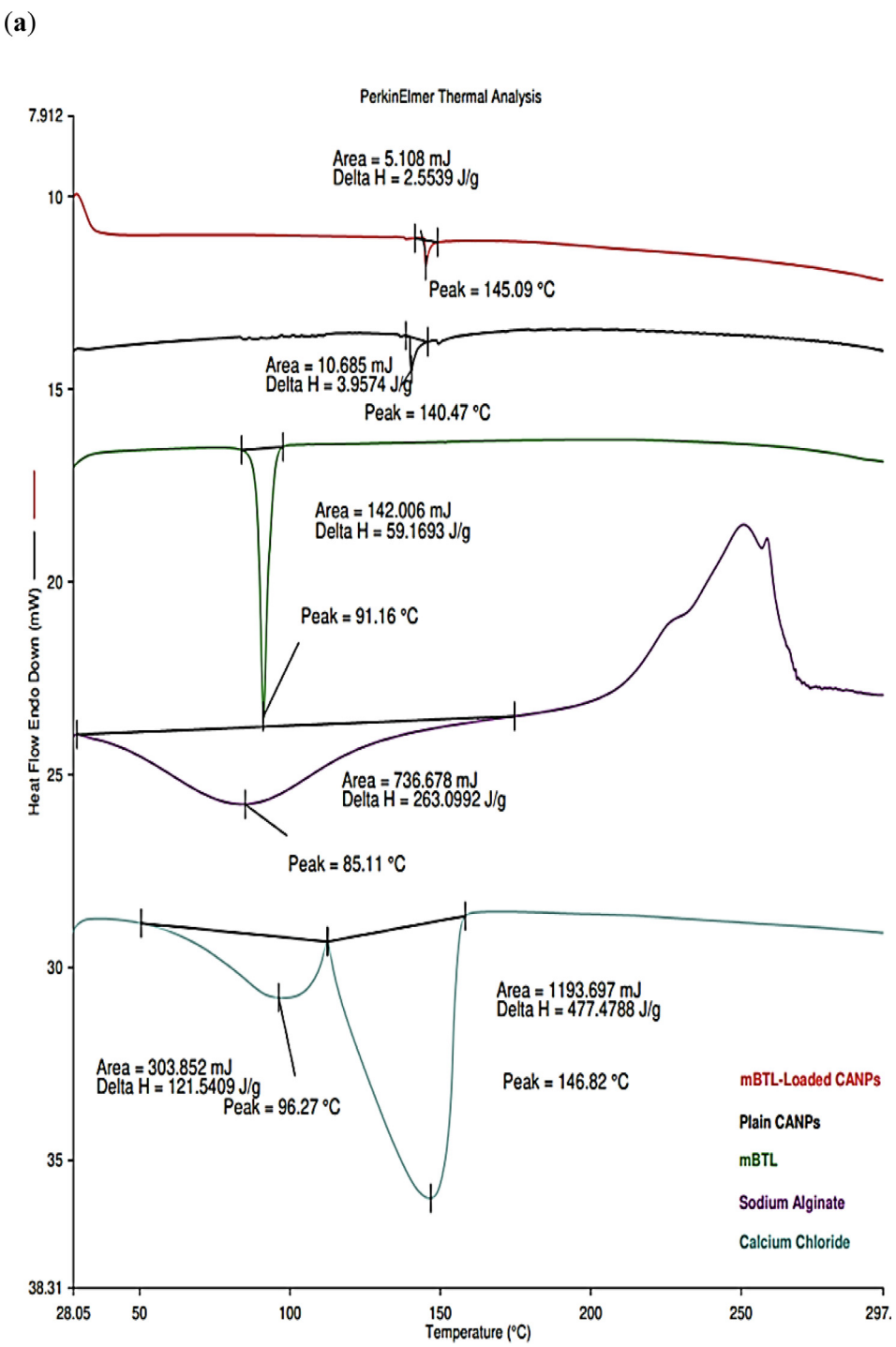

Fig. 5. The DSC Thermogram s of calcium chloride, sodium alginate, free mBTL, plain CANPs and mBTL-loaded CANPs. (a) representative for all compared thermogram. (b) scaled-up thermogram for mBTL-loaded CANPs.

and shifted temperature to 138.44 °C, further indicate that there is no chemical interaction between the free mBTL and physical mixture.

3.5. Physical stability

The stability of plain CANPs and mBTL-loaded CANPs either in solution or lyophilized mBTL-loaded CANPs under different of temperature conditions at room temperature (25 ± 1 °C), 4 ± 0.5 °C and the lyophilized mBTL-loaded CANPs (frozen sample) was kept at −30 ± 1 °C for 9 month. The samples were tested at predetermined time intervals, 4 months and 9 months. Average PS, PDI and ζ potential of plain and mBTL-loaded CANPs. The effect of time on the stability of average PS of nanoparticles with varying temperatures summarized in Table 2.

At room temperature, the ζ potential of plain and mBTL-loaded CANPs were found to decrease from −21.1 to −39.8 mv and increase from −45.7 to −30.3 mv, respectively after 4 months.

(b)

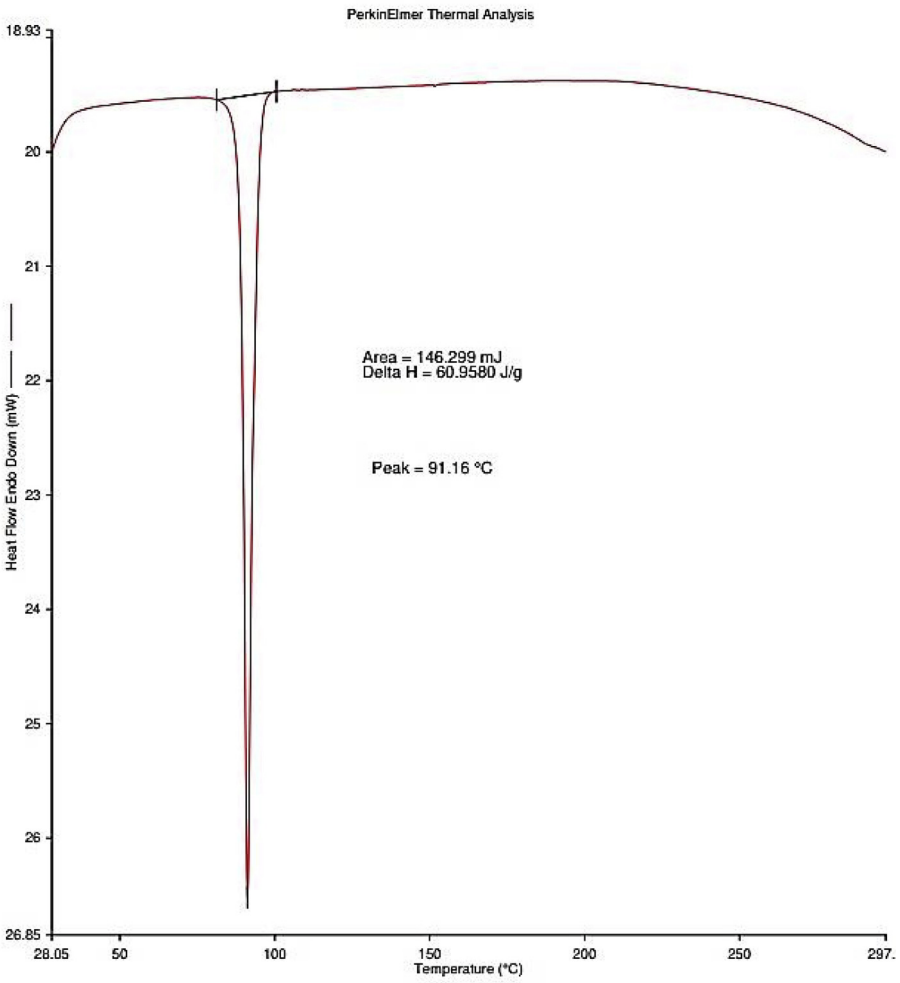

Fig. 5 (*continued*)

Table 2
Effect of time on the Stability of *ζ potential* Nanoparticles at different temperatures.

Physical characterization	Duration	plain CANPs at 25 ± 1 °C	mBTL-loaded CANPs at 25 ± 1 °C	plain CANPs at 4 ± 0.5 °C	mBTL-loaded CANPs 4 ± 0.5 °C	Lyophilized plain CANPs at −30° ± 1 °C	Lyophilized mBTL-loaded CANPs −30° ± 1 °C
Z average diameter (nm) ± SD	4 months	155.86 ± 6.29	186 ± 15.70	232.3 ± 6.3	299.83 ± 21.14	267.93 ± 25.41	308.53 ± 15.38
Polydispersity Index (PDI) ± SD		0.483 ± 0.040	0.381 ± 0.061	0.352 ± 0.019	0.423 ± 0.044	0.340 ± 0.028	0.385 ± 0.038
Zeta potential (Mv) ± SD		−39.8 ± 3.39	−47.5 ± 3.10	−36.93 ± 0.899	−42.9 ± 2.09	−30.3 ± 0.962	−37.8 ± 0.355
Z average diameter (nm) ± SD	9 months	205.03 ± 9.73	238.03 ± 38.68	226.7 ± 21.73	222.53 ± 16.40	221.1 ± 51.09	362.7 ± 10.52
Polydispersity Index (PDI) ± SD		0.5206 ± 0.013	0.545 ± 0.009	0.450 ± 0.028	0.370 ± 0.007	0.452 ± 0.045	0.428 ± 0.030
Zeta potential (Mv) ± SD		−40.6 ± 1.34	−27.23 ± 1.47	−35.95 ± 0.05	−35.96 ± 1.50	−43.8 ± 2.66	−47.4 ± 3.42

4. Discussion

Polymeric nanoparticles have been widely implemented due to their clinical usages as delivery systems (Hu et al., 2002, Pressly et al., 2007, Sarmento et al., 2007). Diversity of polymers can be chosen and in this study calcium alginate was chosen as it reveals properties of biocompatibility, biodegradability, viscosity and the ability of gelation with multivalent cations and good bacterial penetration (Rajaonarivony et al., 1993, Jianlong et al., 1999). Since QS coordinate bacterial communities and their pathogenic activities including; protease activity, pyocyanin production, hemolysis and biofilm development through cell–cell communication using small diffusible signal molecules, disruption of QS interferes with virulence factors formation and maturation inhibitors (Hentzer et al., 2003, Amara et al., 2009, O'Loughlin et al., 2013).

The synthesized CANPs were loaded with QSI mBTL and characterized for the size, charge and distribution of the formulated nanoparticles. The loading capacity of CANPs showed around 93.21% ± 0.045 of encapsulated mBTL. The synthesized mBTL-loaded CANPs showed sizes (150–200 nm) similar to those of *Pseudomonas bacteriophages* (Cui et al., 2016), with negative surface charge indicating the simple uptake of these NPs by the bacterium. The comparison of TEM images of plain CANPs to mBTL-loaded NPs showed smooth nano-size spherical to irregular shapes, respectively. TEM examination of these nanoparticles provide further validation as proper carriers because of their desirable properties (size and high surface area) (Hu et al., 2002). The in vitro mBTL release patterns from the CANPs were evaluated at pH 7.4 at 37 ± 0.5 °C, over 48 h resembling ambient biological conditions. Fig. 2 depicted higher cumulative sustained flow pattern of mBTL from CANPs. The percentage release of the mBTL from CANPs showed a higher cumulative release over 24 h (80.13 ± 0.034), followed by gradual increase release pattern of mBTL (95.27 ± 0.032 within 48 h). The results were compared to the fast and complete release of free mBTL (100 % ± 0. 015) freely diffused through membrane within 7 h, as no factor hinder the release through the membrane. The slow release profile of mBTL from loaded-CANPs attributed to overcoming it's entrapment in the hydrophobic core along with the protonation of –COOH in alginate, weakening the electrostatic interaction between mBTL and alginate.

FTIR was used to confirm loading mBTL into CANPs. This was achieved by presence of the band at 1656.66 cm^{-1} which is corresponding to thiolactone ring stretching vibration in mBTL and appeared in mBTL-loaded CANPs.

The DSC analysis showed intact physical state of loaded mBTL into CANPs indicated by initial two endothermic peaks at 96.27 °C, 146.82 °C of calcium chloride and one endothermic peak at 85.11 °C. The thermogram of mBTL showed a characteristic sharp exothermic single peak around 91 °C also, the endothermic peak of physical mixture appeared to be combination of calcium chloride and sodium alginate was registered at 140.47 °C. The free mBTL peak was appeared and distinguished in thermogram of mBTL-loaded CANPs and increase in melting point of free mBTL and shifted temperature to 138.44 °C, furtherly indicate that there is no chemical interaction between the free mBTL and physical mixture.

Stability test of encapsulated mBTL in CANPs were evaluated over a period of 4 and 9 months at various temperature ranges. The release mBTL from CANPs formula showed intact and stable with similar released pattern were observed, however, slight increase in the particle size of both plain CANP and mBTL-loaded-CANPs detected and can be attributed to aggregation of NPs that sediment with time. With further future microbiological assessment, the data might suggest that the mBTL-loaded-CANPs may be an alternative potential delivery system of quorum sensing inhibitors to *Pseudomonas aeruginosa*.

5. Conclusions

The quorum sensing inhibition strategy is a broadly accepted anti-virulence mechanism. The developed *meta*-bromo-thiolactone calcium alginate nanoparticles and the inhibition of QS mediators might be a potential evolutionary alteration that can decrease the resistance of the fouling bacteria. Therefore, further microbiological studies are required to demonstrate the mechanisms of action and the optimal amounts of the *meta*-bromo-thiolactone calcium alginate nanoparticles quorum sensing inhibitory that are safe and applicable.

6. Author Contributions

FSA and FYA: Conceptualization, design of study, acquisition of data, validation, supervision and writing final draft preparation. EKE: Acquisition of data, analysis of data, visualization, interpretation of data and writing first draft preparation. HA chemical synthesis and analysis of mBTL and interpretation of all chemical analysis. RA and IA: Resources, visualization, and interpretation of data, writing- reviewing, and editing. All authors have read and agreed to the published version of the manuscript.

7. Funding

This research project was supported by Researchers Supporting Project number (RSP-2021/340), King Saud University, Riyadh, Saudi Arabia.

Data Availability Statement

Data will be available by the correspondence upon request.

Declaration of Competing Interest

The authors declare that they have no known competing financial interests or personal relationships that could have appeared to influence the work reported in this paper.

Acknowledgments

This research project was supported by Researchers Supporting Project number (RSP-2021/340), King Saud University, Riyadh, Saudi Arabia.

References

Amara, N., Mashiach, R., Amar, D., et al., 2009. Covalent inhibition of bacterial quorum sensing. J. Am. Chem. Soc. 131, 10610–10619.
Baselga, R., Albizu, I., De La Cruz, M., et al., 1993. Phase variation of slime production in Staphylococcus aureus: implications in colonization and virulence. Infect. Immun. 61, 4857–4862.
Bayer, A.S., Park, S., Ramos, M.C., et al., 1992. Effects of alginase on the natural history and antibiotic therapy of experimental endocarditis caused by mucoid Pseudomonas aeruginosa. Infect. Immun. 60, 3979–3985.
Bayer, A.S., Speert, D., Park, S., et al., 1991. Functional role of mucoid exopolysaccharide (alginate) in antibiotic-induced and polymorphonuclear leukocyte-mediated killing of Pseudomonas aeruginosa. Infect. Immun. 59, 302–308.
Bhatt, P., Fnu, G., Bhatia, D., et al., 2020. Nanodelivery of resveratrol-loaded PLGA nanoparticles for age-related macular degeneration. AAPS PharmSciTech. 21, 1–9.
Christiani, T.R., Toomer, K., Sheehan, J., et al., 2016. Synthesis of thermogelling poly (N-isopropylacrylamide)-graft-chondroitin sulfate composites with alginate microparticles for tissue engineering. JoVE (Journal of Visualized Experiments) e53704.
Cui, X., You, J., Sun, L., et al., 2016. Characterization of Pseudomonas aeruginosa phage C11 and identification of host genes required for virion maturation. Sci. Rep. 6, 1–14.

Danese, P.N., Pratt, L.A., Kolter, R., 2000. Exopolysaccharide production is required for development of Escherichia coli K-12 biofilm architecture. J. Bacteriol. 182, 3593–3596.
Gellatly, S.L., Hancock, R.E., 2013. Pseudomonas aeruginosa: new insights into pathogenesis and host defenses. Pathogens Disease. 67, 159–173.
Gomathi, T., Susi, S., Abirami, D., et al., 2017. Size optimization and thermal studies on calcium alginate nanoparticles. IOSR J. Pharm., 1–7
Govan, J.R., Deretic, V., 1996. Microbial pathogenesis in cystic fibrosis: mucoid Pseudomonas aeruginosa and Burkholderia cepacia. Microbiol. Rev. 60, 539–574.
Hentzer, M., Wu, H., Andersen, J.B., et al., 2003. Attenuation of Pseudomonas aeruginosa virulence by quorum sensing inhibitors. The EMBO J. 22, 3803–3815.
Hu, Y., Jiang, X., Ding, Y., et al., 2002. Synthesis and characterization of chitosan–poly (acrylic acid) nanoparticles. Biomaterials 23, 3193–3201.
Jianlong, W., Horan, N., Stentiford, E., et al., 1999. The radial distribution and bioactivity of Pseudomonas sp immobilized in calcium alginate gel beads. Process Biochem. 35, 465–469.
Lee, D.G., Urbach, J.M., Wu, G., et al., 2006. Genomic analysis reveals that Pseudomonas aeruginosa virulence is combinatorial. Genome Biol. 7, 1–14.
Li, P., Dai, Y.-N., Zhang, J.-P., et al., 2008. Chitosan-alginate nanoparticles as a novel drug delivery system for nifedipine. Int. J Biomed. Sci.: IJBS. 4, 221.
Libo, W., Zhang, J., Watanabe, W., 2011. Physical and chemical stability of drug nanoparticles. Adv. Drug Deliv. Rev. 63, 456–469.
Liu, J., Xiao, J., Li, F., et al., 2018. Chitosan-sodium alginate nanoparticle as a delivery system for ε-polylysine: Preparation, characterization and antimicrobial activity. Food Control 91, 302–310.
Monday, S.R., Schiller, N.L., 1996. Alginate synthesis in Pseudomonas aeruginosa: the role of AlgL (alginate lyase) and AlgX. J. Bacteriol. 178, 625–632.
O'Loughlin, C.T., Miller, L.C., Siryaporn, A., et al., 2013. A quorum-sensing inhibitor blocks Pseudomonas aeruginosa virulence and biofilm formation. Proc. Natl. Acad. Sci. 110, 17981–17986.
Pressly, E.D., Rossin, R., Hagooly, A., et al., 2007. Structural effects on the biodistribution and positron emission tomography (PET) imaging of well-defined 64Cu-labeled nanoparticles comprised of amphiphilic block graft copolymers. Biomacromolecules 8, 3126–3134.
Rajaonarivony, M., Vauthier, C., Couarraze, G., et al., 1993. Development of a new drug carrier made from alginate. J. Pharm. Sci. 82, 912–917.
Sarmento, B., Ferreira, D., Jorgensen, L., et al., 2007. Probing insulin's secondary structure after entrapment into alginate/chitosan nanoparticles. Eur. J. Pharm. Biopharm. 65, 10–17.
Sarmento, B., Ferreira, D., Veiga, F., et al., 2006. Characterization of insulin-loaded alginate nanoparticles produced by ionotropic pre-gelation through DSC and FTIR studies. Carbohydr. Polym. 66, 1–7.
Smith, R.S., Iglewski, B.H., 2003. Pseudomonas aeruginosa quorum sensing as a potential antimicrobial target. J. Clin. Investig. 112, 1460–1465.
Thomas, D., Nair, V.V., Latha, M., et al., 2019. Theoretical and experimental studies on theophylline release from hydrophilic alginate nanoparticles. Future J. Pharmaceut. Sci. 5, 1–7.
Yan, J., Guan, Z.-Y., Zhu, W.-F., et al., 2020. Preparation of puerarin chitosan oral nanoparticles by ionic gelation method and its related kinetics. Pharmaceutics. 12, 216.
Yildiz, F.H., Schoolnik, G.K., 1999. Vibrio cholerae O1 El Tor: identification of a gene cluster required for the rugose colony type, exopolysaccharide production, chlorine resistance, and biofilm formation. Proc. Natl. Acad. Sci. 96, 4028–4033.